

ADDITIVE MANUFACTURING WITH LIQUID LATEX AND RECYCLED END-OF-LIFE RUBBER

Miguel Angel Quetzeri Santiago (+ *Co-first author*)

Clara Louise Hedegaard (+ *Co-first author*, * *Corresponding author*)

Jose Rafael Castrejón-Pita
r.castrejonpita@qmul.ac.uk

School of Engineering and Materials Science, Queen Mary University of London
Mile End Road, E1 4NS, London, UK

Abstract

Elastomers and rubber are common industrial materials used for test objects, supporting parts, and many other commercial products. The industrial processing of these materials is currently dominated by injection moulding, which reduces manufacturing costs, and speeds up production. However, this manufacturing method does not permit personalisation or customisation, and lacks the versatility of other techniques such as 3D printing. Understandably, there has been a move towards additive manufacturing (AM) with elastomers. This work proposes a new approach to AM with liquid latex, using a drop-on-demand (DoD) based inkjet to fabricate latex patterns. The print-head actuator benefits from a higher material compatibility compared to conventional inkjet/extrusion-based printers, allowing the jetting of viscous fluids as well as liquids with high solids loading. The set-up allows printing with viscous liquid latex of a high solid content (60 wt. %). The process is controllable and reliable, making the printing of patterns possible. Additionally, we explore printing with micronized rubber powder (MRP) made from end-of-life tires, to test solid-particle loading compatibility, and as a novel method for rubber recycling. Here, we demonstrate that large scale DoD inkjet printing is capable of handling solid particle loadings of up to 10 wt. % in addition to the high solid content liquid latex. Moreover, multi-layer objects were created from pure liquid latex as well as from MRP/latex suspensions. Material characterisation indicates that the stiffness of cured latex is not altered by the addition of MRP but reduces the maximum elongation length from 750% to 430%. The results highlight the ability to print with both high particle loading and large particles. This explorative study demonstrates the potential of AM processes with liquid latex as well as a new approach to tire rubber reuse.

Keywords

3D printing, Rubber, Latex, Recycling, Multi-material printing, Drop-on-Demand

Introduction

Rubber and elastomers are widely used materials in industry¹ owing to their advantageous physical properties; good chemical and structural stability, heat resistance and thermal insulation capability, and high strength to weight ratio². Traditional manufacturing with elastomers is often done by moulding and casting. This process allows for little design flexibility, permits mass production but is not flexible to produce one-off products. As such, there has been a move towards developing additive manufacturing (AM) techniques for elastomer/rubber production. For example, thermoplastic elastomers have been fabricated using laser sintering³⁻⁵, however the resultant structures were found to have reduced mechanical properties compared to rubber objects fabricated via the conventional route. Liquid silicone elastomers have been printed using extrusion based methods⁶ but this

method cannot be applied to a wide range of elastomers due to the restrictions in viscosity. An alternative AM method for liquid elastomers is drop-on-demand (DoD) inkjet printing.

DoD inkjet printing allows droplets to be ejected onto a substrate and subsequently cured. Droplets are conventionally placed adjacently to each other to allow them to coalesce and form a uniform straight array. The z-axis definition is created by overlaying layers, with intermittent curing or crosslinking steps to ensure adequate support of subsequent layers. In DoD printing, a pressure pulse induced by thermal, piezoelectric or acoustic actuation causes a liquid droplet to form and jet from the print-head nozzle. DoD has a number of advantages above other AM technologies; firstly, there is no substrate contact, avoiding contamination of the nozzle, and secondly, higher printing speeds can be achieved compared with for example fused deposition modelling (FDM)⁷. Moreover DoD methods allow a greater control and variability of the droplet volume and speed^{8,9}. In addition, it is a digital technology with great flexibility that naturally permits personalisation and one-off production. Unfortunately, material compatibility is an issue in commercial inkjet systems as the technology is restricted to operate under a narrow window of liquid viscosities.

Recent advanced in the field, includes examples of the rubber latex being successfully printed using inkjet; Raza *et al.* used a commercially available Microfab print-head to print low melting point alloys and elastomers¹⁰, and Lukić *et al.* printed diluted liquid latex (35 wt. % solid content) with a commercially available piezoelectric inkjet printer⁵. Whilst these examples show that progress has been made, the techniques still suffer from similar limitations in ink viscosity, solid content, nozzle clogging, and agglomeration. In addition, inks used in AM methods have additional requirements to that of deposition resolution, as droplets are required to cure or solidify fast and leave an adequate footprint to build definition in the z-axis. These restrictions still need to be addressed to improve 3D printed objects made from viscous or high solid content materials such as bio-gels, conductive inks, and liquid latex.

From the limitations in DoD printing, solid particle loading is one of the main limitations across all inkjet industries. The industry standard for conventional inkjet is a maximum viscosity of 20 cP with a solids loading of < 10 % per volume, and a particle diameter of no greater than 1/20 of the nozzle diameter^{5,7,11,12}. Whilst being able to inkjet un-diluted liquid latex is an interesting prospect in itself, the ability to add solid particles to form a colloidal ink widens the market applications for this technique. The addition of particles can be used to reinforce the positive mechanical properties or improve other properties such as thermal and electric conductivity, stiffness or elasticity of a given construct. Moreover, this includes the possibility of reusing discarded rubber materials, in form of micronized rubber powder (MRP), in the manufacturing of new products.

In recent years, there has been a move towards producing MRP from waste materials such as tires. Tires remain a major source of waste, despite an increase in governmental initiatives to promote their recycling. In the USA alone there are still 67 million tires occupying landfills, and an estimate of 25 % (2010) of all end-of-life tires are placed into landfills worldwide¹³. Currently, a mere 10 % of end-of-life tires are recycled to create new products¹³. A reason for the low rate is the lack of suitable recycling methods and the limited ability to make new products with discarded material. MRP has proved to be environmental friendly as it can be obtained mechanically with no contaminants released to the environment. The benefits, in terms of cost have been previously demonstrated for manufacturing with MRP, to create moulded and extruded products¹⁴⁻¹⁷.

In this study, we propose to inkjet print with liquid latex, with and without MRP, as a step towards cheaper mould manufacturing with elastomer/rubber based materials. We introduce a versatile DoD inkjet print-head capable of printing pure liquid latex containing a 60 wt. % solid content and a liquid viscosity of 21.8 ± 0.2 cP. Moreover, we explore the concept of creating hybrid MRP/latex constructs by using colloidal inks of latex and MRP. Our results show that, in this instance, the inclusion of MRP does not affect the stiffness of the cured product. Finally, we demonstrate that this ink can be used to manufacture cured latex patterns by DoD deposition and natural curing.

1. Materials and Methods

INK COMPOSITION

Two types of ink formulations were used in this study; pure liquid latex and liquid latex with a suspension of rubber tire waste or fine rubber powder (parlon powder). Pure liquid latex was acquired from Liquid Latex Direct, UK. The liquid latex contains 60 % natural rubber, 40 % water and < 0.3 % ammonia. The density was measured to be $940 \pm 50 \text{ mg}\cdot\text{mL}^{-1}$ and the viscosity to $21.8 \pm 0.2 \text{ cP}$. Suspensions were made using parlon powder and thereafter with a coarse rubber powder made from of end-of-life rubber, namely, micronized rubber powder (MRP). Suspensions were made by dispersing the parlon powder or MRP in undiluted liquid latex. The weight percentage of suspended MRP or parlon powder was calculated as $W_{\text{MRP}}/(W_{\text{L}}+W_{\text{MRP}})$ or $W_{\text{P}}/(W_{\text{L}}+W_{\text{P}})$, where W_{MRP} , W_{P} and W_{L} refer to the weight of MRP, parlon powder and undiluted liquid latex respectively. Synthetic white parlon powder was purchased from IONXIA, UK (~66 % chlorine and < 2.5 % toluene) and MRP was kindly provided by Artis UK. A heterogeneous mixture of MRP was used with a maximum particle size of 0.6 mm. Parlon powder was suspended at concentrations of 3.5 to 6.7 wt. %. MRP was suspended at the concentration 9.6 wt. % when used for printing. Mechanical testing was carried out on cast and cured latex samples containing MRP at concentrations 0, 5, 9 and 16 wt. %.

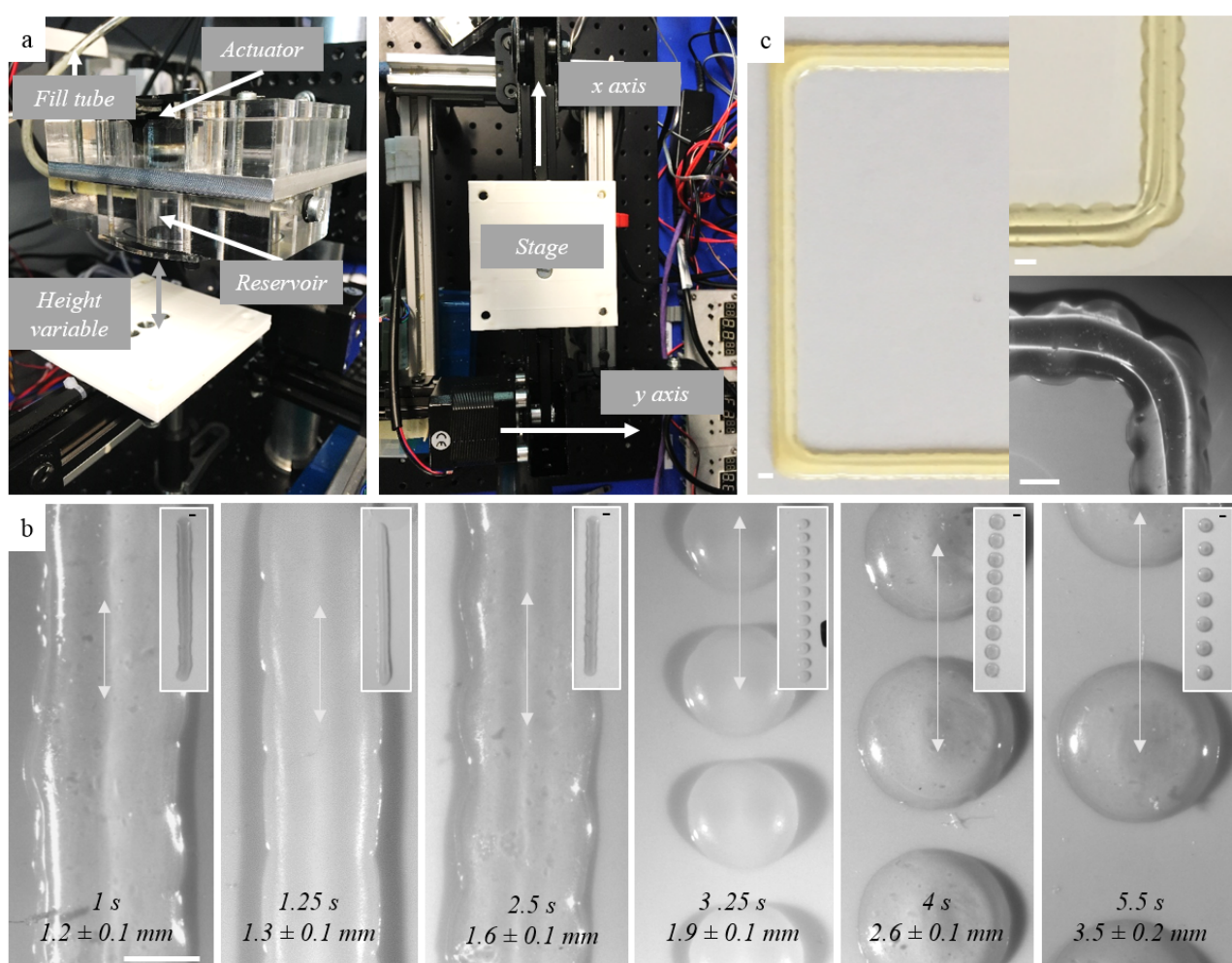


Figure 1. Printing with liquid latex. (a) The experimental set-up showing the GRBL controlled stage and the print-head mounting (The 9 mL reservoir print-head is shown); (b) Varying the droplet interval keeping the pulse signal and nozzle diameter constant: from left to right increasing the interval length from 1 s to 5.5 s (inserts show birds-eye perspective); (c) An example of a single layer structure made from pure liquid latex, using a droplet interval of 2.5 s with two close-ups of the corner resolution. (All scale bars 1 mm.)

PRINT-HEAD DESIGN

For our experiments, two print-head designs were used. These were manufactured in-house and use loudspeaker as actuators. In both systems, the actuator, driven by a pulse generator, pushes the liquid through the nozzle to create a droplet. The print-heads are fed with fresh ink through an attached syringe which in turn is attached to a fast-acting meniscus controller (Inca Digital Printers Ltd., UK) used to balance the pressure inside the print-head and the atmospheric pressure, keeping the meniscus pinned at the nozzle. In this manner, a single pulse of pressure generates a single drop. Two print-head sizes were used to assess their performance with the colloidal inks. The small print-head uses a 20 mm diameter loudspeaker (8 Ohms, 0.1 W), has an inner liquid reservoir volume of 4 mL, and a conical nozzle with an outer diameter of 1.0 mm. The larger print-head uses a Visaton Structure-Borne Driver loudspeaker (8 Ohms, 25 W) with a 9 mL volume reservoir, and a 0.85 mm conical nozzle. We claim that these drivers (loudspeakers) have more actuation power than other piezoelectric driven print-heads, e.g. MicroFab and MicroDrop, so making the printing of high viscosity liquids a reality. The driving signals on both systems are produced using a TTI pulse generator, an acoustic amplifier, and recorded by a digital oscilloscope. The waveform is kept to a single pulse, with control over the pulse amplitude and width, to adjust the droplet speed and size. These print-head designs are further developments (miniaturization and simplification) of a system presented elsewhere¹⁸.

EXPERIMENTAL SETUP

The small print-head was mounted on to a 2D motorised stage while the substrate (Kodak inkjet paper) was secured to a support at a fixed distance. In contrast, the larger print-head was fixed to a vibration damped support and the substrate mounted onto the stage (Figure 1a). The printing distance, i.e. the distance from the print-head to the substrate, was kept constant at approximately 5 mm for both systems. The stages were operated by stepper motors and controlled by the GRBL protocol. In brief, the GRBL code transforms a digital structure into coordinates and a series of orders that control the motion of the stepper motors and trigger the jetting of the print-head. The jetting trigger activates (gated mode) the pulse generation signal that is sent to the speaker to print on demand. The GRBL properties, stepper speed, and printing frequency were adjusted to obtain a placement resolution below ~ 300 μm . Both meniscus controllers were set to a negative pressure in the range of 8-9 mm H₂O to keep the meniscus pinned at the nozzle and avoid flooding.

THREE-DIMENSIONAL PRINTING TECHNIQUE

The following procedure was followed for printing; Initial loading of print-head and syringe followed by adjusting the backpressure. The driving signal for droplet formation was adjusted in terms of pulse duration and intensity for each ink composition. The printing speed and frequency could be adjusted for each ink and system so that droplet placement could coalesce and form a continuous line, or form a string of equally spaced separated droplets. Two-dimensional patterns were created by controllably printing on the substrate, and three-dimensional constructs were attempted by overlaying consecutive printing layers. Two methods of drying were tested, i) ambient air curing where individual ~ 1.0 mm width layers take up to 4 min to solidify, and ii) blowing hot air (~ 400 C from a 2.3 W heat gun) onto the individual print layers for 10 s to achieve curing of the pattern surface.

IMAGING

Air dried constructs and ink samples were imaged using standard bright field microscope from Leica Instruments, USA (Leica MZ12.5 Stereomicroscope with an external light source Leica CLS150X). All standard microscopy images were analysed using the software ImageJ, with at least five measurements taken per determined value (for example construct and droplet dimensions).

MATERIAL CHARACTERISATION

An indentation test was run on cast samples (Figure 2e) containing varying concentrations of MRP (0, 5, 9 and 16 wt. %) to determine the effects of rubber on the material stiffness. Three different samples per concentration were tested, with 2-3 tests on each sample, hence a minimum of 8 tests per concentration. The Young's modulus,

E , was derived from the resulting force-displacement data. Tensile testing was carried out on printed pure liquid latex samples (1 layer and 4 layer), as well as on cast latex samples containing varying amounts of MRP (0, 5, 9 and 16 wt. %). All samples tested were of a rectangular shape. The experiments were carried out on an Instron 5566 UTM with a $\pm 100\text{N}$ static load cell and a constant strain rate of 30 mm/min. The tensile stress and strain at the breaking point were determined from the data, as well as the Young's modulus. A minimum of 2 samples were tested per concentration. All geometries for the tensile test, and the values for the obtained strain, stress and Young's modulus can be found in Table 1. Representative stress-strain plots are shown in Figure 3. Statistical analysis was carried out using the software GraphPad Prism 5. A one-way analysis variance (ANOVA) was used, and a statistical significance was accepted when $p \leq 0.05$.

	L_0	W	T	Strain at failure	Stress at failure	Young's Modulus*
	<i>mm</i>	<i>mm</i>	<i>mm</i>	<i>mm/mm</i>	<i>MPa</i>	<i>MPa</i>
Control (0 wt. %)				75.1 ± 3.1	7.9 ± 0.1	2.7 ± 0.2
5 wt. %				51.5 ± 24.3	7.51 ± 2.1	2.1 ± 0.5
9 wt. %	2.3 ± 0.6	8.2 ± 0.5	0.5 ± 0.1	48.5 ± 6.9	7.68 ± 1.9	2.4 ± 0.4
16 wt. %				48.1 ± 1.9	5.44 ± 2.0	2.5 ± 0.7
Control Thin	5.9	1.0	0.2	-	-	1.6
1 Layer Print (1LP)	2.3 ± 0.3	1.9 ± 0.2	0.3 ± 0.3	43.4 ± 5.7	13.5 ± 2.1	1.5 ± 0.1
4 Layer Print (4LP)	2.1 ± 0.5	3.5 ± 0.2	1.0 ± 0.1	55.3 ± 4.9	5.8 ± 0.1	4.0 ± 0.8

TABLE 1. Summary table of the samples used for tensile testing and the determined strain and stress values at the breaking point. All values reported are mean \pm standard deviation. *The Young's modulus is reported as the average from the indentation and tensile tests.

Results and Discussion

INKJET PRINTING WITH LIQUID LATEX

Initial tests were focused on establishing reliable printing conditions with pure liquid latex, evaluated in terms of droplet formation and reproducibility, as well as jetting stability over time. Pulse signals were adjusted by changing the pulse width and voltage, to obtain fully formed droplets and avoid satellite droplets¹⁹. Conical nozzles were used in both printing systems, leading to droplets of uniform size both in-flight and post impact. We have previously shown that our systems can produce droplet speeds in the range of 0.5-2.0 m.s⁻¹, where droplet creation was dependent on the ink properties, the nozzle geometry, and the signal voltage and width¹⁸. Repetition rates were restricted by the nozzle re-filling time, i.e. the time taken by the meniscus controller and surface tension to "fill" the missing/jetted liquid at the reservoir. Given the high viscosity of the liquid latex, a droplet deposition rate (linear printing speed) of 0.15 cm s⁻¹ was used. Our results indicate that latex droplets produce a footprint (printing dot size) of twice its original diameter, i.e. a droplet from a 1.0 mm nozzle produces a circular dot footprint of a 2.2 ± 0.9 mm diameter. Within a range, the droplet size can be adjusted by modifying the pressure pulse width and amplitude, without having to change the nozzle diameter. Both print-heads were shown to be capable of jetting pure liquid latex, obtaining consistent jetting with liquid latex containing 60 wt. % solid content and of relatively high viscosity (21.8 ± 0.2 cP). In conventional DoD printing, often a critical droplet spacing is defined by which the droplets are close enough to coalesce forming a parallel sided line. Above and below the critical spacing, either bulging of the line or no coalescence occurs respectively²⁰. Figure 1b shows the range of droplet intervals tested, keeping the motor speed and nozzle diameter constant. As evident, the deposited latex droplets remain isolated (un-coalesced) at droplet jetting intervals greater than 2.5 s, whilst reducing the interval to ≤ 2.5 s leads to droplet coalescence and path formation. At smaller droplet jetting intervals, the increased overlap leads to instability and bulging.

Under our jetting conditions, continuous printing of pure liquid latex was shown to be consistent and reliable over periods of up to 1 hour. Figure 1c shows the left-side of a square pattern fabricated with the larger print-head and using a droplet jetting interval of < 2.5 s. These vertical and horizontal lines demonstrate the accuracy and stability of the print. The two close-ups seen in Figure 1c show examples of the achievable resolution at the corners. Printing at corners was controlled by adding a gap at the turning point to minimise bulging from the potential three-way droplet coalescence, i.e. the corner droplet, and the neighbouring droplets in the horizontal and vertical direction.

Curing at the nozzle is an important limitation for inkjet printing. Whilst a small nozzle is desired to produce small drop sizes that dry fast, a small sessile meniscus can cure itself at the print-head during idle times. In fact, we observed cured menisci blocking nozzles within minutes of stopping printing. In our experiments, cleaning the nozzle plate with a fibre-free swab was sufficient to unblock the meniscus. In a commercial application, nozzle unblocking can potentially be done by flushing out the cured meniscus prior to printing.

COLLOIDAL CONSTRUCTS AND INKS

In AM, a degree of versatility in the ink composition is often needed to meet the end product specifications. Ink formulation normally rely on the addition of solid particles to alter the properties of the end product, such as reinforce the material strength and durability, or to add colour using pigments. Restrictions in solid particle loading is a well-known problem in inkjet technology, with conventional printing inks containing < 10 wt. % solid residue⁸. Having already shown that the developed system is capable of printing with pure liquid latex of a high solid content, the next step was to prove the feasibility of printing with a suspension of undiluted liquid latex with the addition of either parlon powder or MRP (colloidal ink suspension). The test was designed to include MRP made from end-of-life tire waste. MRP is a heterogeneous mixture of rubber, and is comparatively crude. As such, preliminary experiments were carried out using fine parlon powder, which has a very narrow size distribution, and an average particle size in the nanometre range. Colloidal ink suspensions of 3.5 and 6.7 wt. % parlon powder were prepared and tested in the print-head. In both instances, consistent jetting was observed (example shown in Figure 2a). The printing of the rubber particle and latex ink was demonstrated by jetting a series of defined arrays as seen in Figure 2a,d. The parlon powder remained suspended in solution throughout the duration of printing, as observed through the printed droplets and when inspecting the leftover ink post printing. The quality of the parlon distribution post printing was analysed using microscopy imaging. The parlon powder was shown to aggregate in the suspension (Figure 2b-c) leading to a non-uniform size distribution of the suspended particles. However, the parlon was shown to be well distributed within the ink, such that all droplets contain a homogenous mixture of liquid latex and parlon powder.

Having shown that a solid loading of fine rubber powder is feasible, our experiments then focused on the jetting of coarse recycled MRP, which is of greater commercial interest due to its recycling potential. The MRP used has an average particle size of 0.6 mm, comparatively larger than the parlon powder but with a narrow size distribution. The parlon powder experiments were repeated using a 9.6 wt. % MRP particle loading. A uniform droplet size was observed throughout each print, although unlike parlon powder, a non-homogenous distribution of MRP was visible post curing. Solid tire rubber could be clearly visualised in ~ 90 % of the droplets. The non-uniform distribution of MRP can be attributed to two factors; similar to parlon powder, the MRP tended to aggregate in solution creating large clusters, and secondly, due to the weight of coarse MRP they were more prone to settle on the bottom of the print-head. This issue is common to all colloidal ink suspensions, and not a property specific to the liquid latex system. In fact, many commercially available print-heads continuously recirculate the ink within the print-head to avoid aggregation and clogging the nozzles^{21,22}. Implementing a more defined and rigours mixing procedure or using smaller particles⁷, could mitigate agglomeration of the particles in solution as well as reducing the observed settling in the print-head. Alternatively, gentle vibration of the print-head reservoir could be introduced.

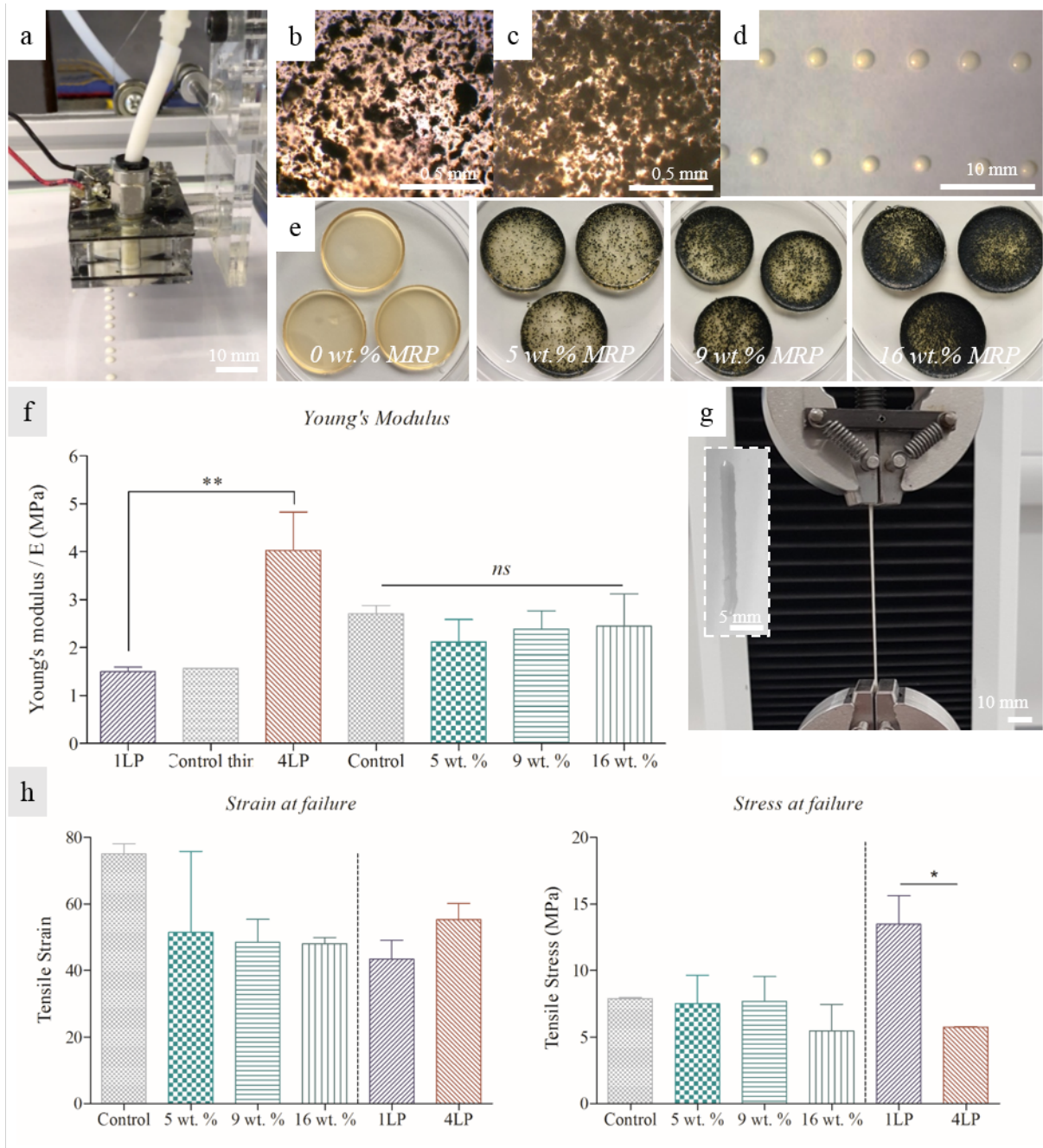


Figure 2. Liquid latex with rubber particle loading. (a) Time-lapse of the print-head mounted to the x/y stage, jetting pure liquid latex (1 drop/1.5 seconds) (scale bar 1 mm); Microscopy images of liquid latex with (b) 3.5 wt. % and (c) 6.7 wt. % parlon loading; (d) A defined array made by jetting liquid latex containing 6.7 wt. % parlon powder; (e) Cast rubber samples of pure liquid latex and with increasing MRP loading (5, 9 and 16 wt. %); (f) A graph of Young's Modulus, determined using indentation and tensile testing, of cast samples with 5, 9 and 16 wt. % MRP (control; 0 wt. % MRP), and printed samples of 1 and 4 layers (1LP and 4LP respectively) (control thin: a pure latex cast). Data reported as mean \pm standard deviation; (g) Example of elongation of a 1 layer printed sample (1LP) under a constant strain tensile test (insert: original sample) and (h) Tensile stress and strain at breaking point, derived from the constant strain tensile experiments. Data reported as mean \pm standard deviation

The impact on the mechanical properties was tested for a range of MRP particle loadings. Samples were prepared using casting, as shown in Figure 2e, with a range of 0 to 16 wt. % MRP solid content. The samples were tested by the standard indentation and constant strain tensile tests. The two experimental methods yielded

comparative values for the Young's Modulus (the overall mean \pm standard deviation are reported in Table 1). The results indicate that the stiffness of these materials are not greatly affected by the colloid content, and any differences are within error of each other and not statistically significant (Figure 2f). However, the tensile test indicates that adding MRP to the latex reduces the maximum elongation length from 750% to 480% (Figure 2h, strain graph). The ultimate tensile stress (stress at the breaking point) was found to be equal, within error, for all 4 sample types (Figure 2h, stress graph). Having determined the impact of MRP on the mechanical properties, next the effect of printing was tested. Two types of printed pure liquid latex samples were tested, namely, a one layer (1LP) and a four layer (4LP) printed rectangle. The stress-strain plots are shown in Figure 3. An example of the one layer print being tested is shown in Figure 2g. Firstly, in terms of stiffness a higher Young's modulus was observed in the case of four layers compared with one layer. However, in both instances the printed samples yield similar Young's modulus to the cast controls. The one layer printed line (Figures 2g and 2h) was elongated by $434 \pm 60 \%$ prior to breaking, whereas the 4 layer printed line (4 layers printed overlaying each other) was elongated by $553 \pm 50 \%$ (Figure 2h). The one layer print showed a higher ultimate tensile stress compared to the 4 layer print (statistically significant). Overall, we can conclude the droplet-to-droplet and layer-to-layer bonding in the printing do not significantly change the mechanical properties of the latex, however there is a clear dependency on sample thickness as seen in the difference of the ultimate tensile stress. Combining these results, we infer that the effect of MRP particles in latex reduces the elasticity without affecting the stiffness of the printed samples. This is in line with other works, such as Mueller et al. in 2017, that have established that the global and local mechanical properties of inkjet manufactured parts can be affected in manufactured mixed-materials parts²³

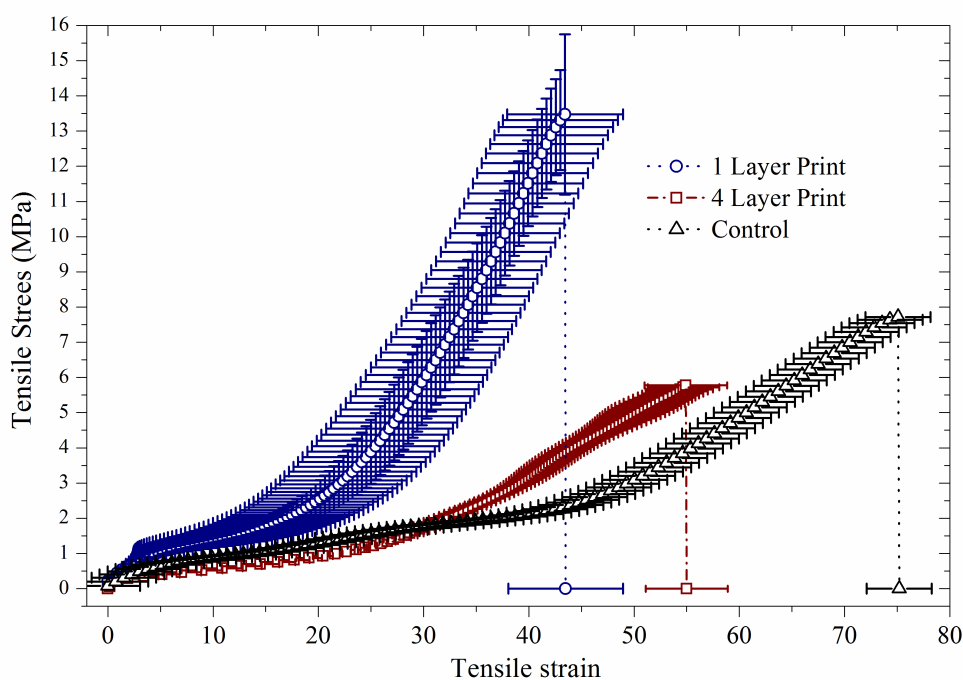


Figure 3. The stress-strain plot for the samples ‘1 Layer Print’, ‘4 Layer Print’ and ‘Control’ (pure latex). All data points are reported as the mean \pm standard deviation

We have demonstrated the ability to print high solid content latex and with suspended recycled rubber, which from an AM perspective brings new possibilities to the recycling potential of rubber tire waste. There is a growing market for commercial AM, with many areas of industry yet to take full advantage of this evidence²⁴. Currently, asphalt and concrete applications where most end of life tires are used or recycled, a maximum of 20 wt. % of rubber is used^{25,26}. In this paper the final 3D printed objects have ≈ 10 wt. % of rubber from tires. However, in contrast to other recycling methods, 3D printing offers a more versatile way of recycling. Despite

having an arguably low quantity of MRP in our ink, this technique can be used in the manufacture of commonly used items, such as for example smartphone cases, in which the market capacity would significantly increase the quantity of recycled rubber per annum. Another possibility is the printing of thermal insulation for circuits or protective coatings on electronic components. Moreover, the system has room for incrementing the rubber tire contents, by for example using finer MRP and/or by diluting the liquid latex. An untested AM option to include a higher MRP content in the final product, can be to print latex on a powder bed 3D printing mode, whereby the liquid latex is used to bind the recycled rubber powder on the bed. In this instance, the MRP would have to be sufficiently fine milled in order for the binding to occur. This method was briefly explored in this study but a purpose build stage would be needed to achieve high-resolution constructs. Other alternative AM techniques, such as fused deposition modelling (FDM) or fused filament fabrication (FFF) are not suitable for manufacturing with tire rubber, as tire rubber does not “fuse” to produce a continuous extruded filament⁵. The system requires further development and optimization to be a solution to the tire waste problem, however this is the first step towards that goal.

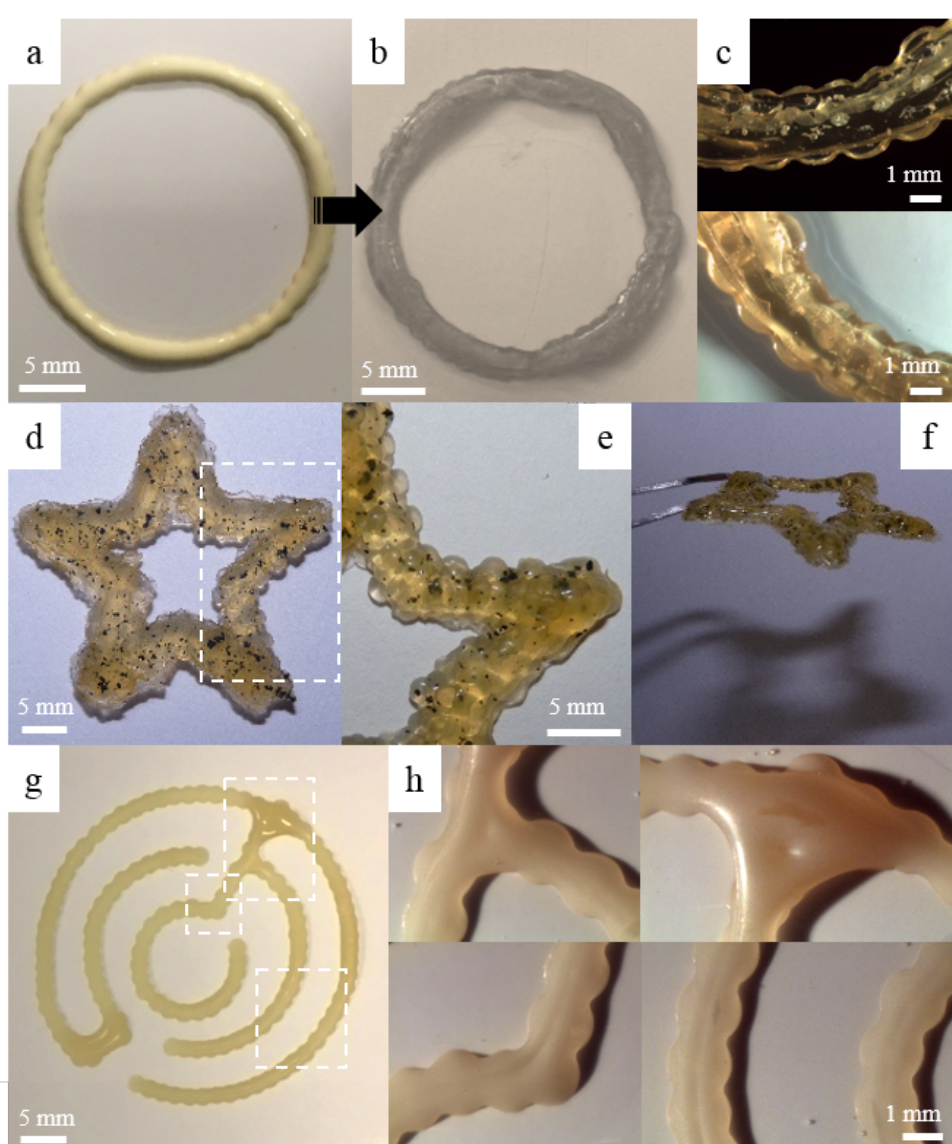


Figure 4. Three-dimensional latex constructs. (a) Three layers of pure liquid latex in wet and (b) dry state, with (c) close-ups of the layer structure; (d) A 3D star construct made from liquid latex with 100 mg/mL (9.6 wt. %) MRP, with (e) close-up of the corners and (f) a side-view; (g) A more complex 1 layer structure made from pure liquid latex and (h) close-ups of the corners and line width

TRANSITION TO THREE-DIMENSIONAL OBJECTS

Having shown that it is possible to print reliably with liquid latex as well as shown the feasibility of using a colloidal ink along with the added material benefits, next the possibility of creating three-dimensional objects was explored. Initially precision and resolution of the system were determined.

In the first instance, pure liquid latex was used. The first patterns created were circles with a diameter of 22 mm (Figure 4a-b), with a droplet interval of 2.5 s to produce a continuous string formation. Three consecutive layers were completed with intermittent hot air blowing allowing each layer to semi-dry before applying the next layer. As previously described, two approaches to drying were tested; firstly, drying under ambient air conditions resulting in 4 min drying time for a ~ 1.0 mm width layer. The second method consisted in blowing hot air (~ 400 C) onto the individual print layers for 10 s to achieve a fast curing of the pattern surface. The print resolution was reduced with increasing layers as evident by the increase in width. This can, for example, be seen in Figure 4a-b, where the wall thickness of the circular pattern increases from 1.7 ± 0.2 mm at layer 1, to 2.6 ± 0.2 mm at layer 3. This effect is also the result of the drying/curing speed as the droplet cures into a spherical cap and not as a pancake shape as in other applications of 3D printing. However, the initial couple of layers retain the precision of the coordinated stage movement and droplet formation, showing that high resolution is achievable. Connecting interfaces were visualised using bright field microscopy. Individual droplets were clearly visualised, showing the layered structure of droplets in the constructs, originating from stepwise layering (Figure 4c). Increasing the speed of drying between layers would increase the resolution retention.

A star pattern (Figure 4d) was made using a 100 mg.mL^{-1} (9.6 wt. %) MRP suspension. The construct thickness measured 1.9 ± 0.4 mm and was made from 15 overlaying layers (Figure 4f). Droplets were in this instance placed adjacent, but not overlapping in an attempt to mitigate the pronounced bulging instability as observed with increasing layers²⁷. Whilst finding the critical droplet spacing is the norm in other 3D inkjet-based printing, in our case the droplets are one order of magnitude larger than conventional DoD. As such, a greater level of precision is potentially achievable when the droplets are kept adjacent without coalescing, allowing for each layer to dry in ‘droplet’ shape. Improving the overall resolution would mean decreasing the nozzle diameter from mm to μm , and thereby increasing control and precision. Smaller DoD systems, such as MicroFab print-heads were available but not tried as the risk of blocking was very high given the size of particles, the high bulk viscosity, and the risk of curing at the nozzle. Post drying the construct revealed an increased aggregation of MRP particles in the pattern, visible as distinctive black patches (Figure 4d-e). At the corners (Figure 4e), the printing resolution also decreases going from an angle of $42 \pm 2^\circ$ to $52 \pm 3^\circ$, meaning that sharpness of each corner is decreased with increasing layers.

Lastly, more complex one-pass printing patterns were attempted using pure liquid latex. Figure 4g-h demonstrate the ability of our technique to create more complex structures, whilst retaining good placement resolution. Zooming in on the connection points (Figure 4h) evidence that whilst a clearly defined three-way corner is possible (top and bottom left), bulging can still occur from three-way coalescence. Further fine-tuning of the meshing GRBL/G-code instructions at the corners can remove this problem by reducing jetting at the corners. Whilst the fluid properties and curing mechanisms require further development to decrease the time of solidification, our results show that single or few layers printing is achievable.

Conclusion

In this paper, we introduce an inkjet based AM process capable of printing with liquid latex with of up to 60 wt. % solid content and a liquid viscosity of 21.8 ± 0.2 cP, both significantly higher than previous printing methods. Moreover, this system is able to print with a mixture of liquid latex and tire rubber particles of 0.5 times the nozzle diameter. Multiple layer objects were fabricated with both pure liquid latex as well as with liquid latex with the addition of MRP. The Young’s modulus as well as the strain at the breaking point showed no change when adding the MRP, while maximum elongation length is reduced. Moreover, the printing process does not affect the Young’s modulus of the objects. The capability of printing with a high particle loading (high solid content latex with the addition of parlon powder or MRP) and a heterogeneous particle size distribution, shows that the print-

head design can operate in a wide range of solid particle loadings. This is a great advance, as most conventional inkjet-based 3D printers cannot operate with viscous liquids or liquids with solid particle loading. The study has demonstrated the potential of AM with liquid latex, however there is still scope for improvement. For example, the drying time of the liquid latex should be shortened further, by for example including a heating source in the stage or in the printing bed. Improvement of the stage and pattern control would enhance the resolution and reliability of the print quality. A reliable method of AM with liquid latex would bring great merits to the industry, by reducing cost of manufacturing (no moulds needed), and adding an unprecedented degree of flexibility in the manufacturing process. Moreover, the study has highlighted a novel method of recycling end-of-life tires. With this work, it is foreseeable that in the future we can create 3D printed objects with rubber tire waste, expanding the current recycling and waste management methods.

Acknowledgements

M. A. Quetzeri Santiago acknowledges the funding from the Mexican Energy Ministry (SENER) and the National Council for Science and Technology (CONACYT) Mexico. We thank Artis UK for providing the micronized rubber powder. We thank Finn Box from the University of Oxford for his support with the indentation tests, and Karen Silva Blankenagel from Queen Mary University of London for her support with the tensile tests.

Author Disclosure Statement

No competing financial interests exist.

References

1. Barlow C, Jayasuriya S, Tan CS. The World Rubber Industry.; 2014.
2. Corporation Woodland Plastics. Understanding Thermoset Plastics. <http://www.woodlandplastics.com/understanding-thermoset-plastics.html>. Published 2015. Accessed June 25, 2018.
3. Goodridge R, Tuck C, Hague R. Laser sintering of polyamides and other polymers. *Prog Mater Sci*. 2012;57(2):229-267.
4. Kruth JP, Levy G, Klocke F, et al. Consolidation phenomena in laser and powder-bed based layered manufacturing. *CIRP Ann - Manuf Technol*. 2007;56(2):730-759.
5. Lukić M, Clarke J, Tuck C, et al. Printability of elastomer latex for additive manufacturing or 3D printing. *J Appl Polym Sci*. 2016;133(4).
6. Duoss EB, Weisgraber TH, Hearon K, et al. Three-dimensional printing of elastomeric, cellular architectures with negative stiffness. *Adv Funct Mater*. 2014;24(31):4905-4913.
7. Guo Y, Huseini SP, Bognet B, et al. Rapid Prototyping Journal Inkjet and inkjet-based 3D printing: connecting fluid properties and printing performance" Inkjet and inkjet-based 3D printing: connecting fluid properties and printing performance. *Rapid Prototyp J*. 2017;23(3).
8. Castrejón-Pita JR, Baxter WRS, Morgan J, et al. Future, opportunities and challenges of inkjet technologies. *At Sprays*. 2013;23(6):541-565.
9. Castrejón-Pita AA, Castrejón-Pita JR, Martin GD. A novel method to produce small droplets from large nozzles. *Rev Sci Instrum*. 2012;83(11).
10. Raza I, Iannucci L, Curtis PT. Introducing a Multimaterial Printer for the Deposition of Low Melting Point Alloys, Elastomer, and Ultraviolet Curable Resin. *3D Print Addit Manuf*. 2017;4(2):83-89.
11. Derby B, Reis N. Inkjet Printing of Highly Loaded Particulate Suspensions. *MRS Bull*. 2003;28(11):815-818.
12. Hon KKB, Li L, Hutchings IM. Direct writing technology-Advances and developments. *CIRP Ann - Manuf Technol*. 2008;57(2):601-620.
13. Forrest M. Recycling and Re-Use of Waste Rubber. Shropshire, England: Smithers Rapra Technology Ltd.; 2014. <http://app.knovel.com/hotlink/toc/id:kpRRWR0002/recycling-re-use-waste/recycling-re-use->

waste.

14. Rubber Manufacturers Association. Scrap Tire Markets in the United States, 9th Biennial Report. Washington; 2009.
15. Aranda Uson A, Ferreira G, Zabalza Bribian I, et al. Study of the environmental performance of end-of-life tyre recycling through a simplified mathematical approach. *Therm Sci.* 2012;16(3):889-899.
16. Kind RC. No Title. In: *Proceedings of RubberCon*. Manchester, UK; 2014.
17. Rosenmayer T, Ayyer R, Papp F. Characterization of Micronized Rubber Powders with cost effective performance benefits in rubber compounds. In: *Annual Technical Conference - ANTEC, Conference Proceedings.*; 2012. <https://www.4spe.org/Resources/resource.aspx?ItemNumber=6359>. Accessed March 7, 2018.
18. Castrejón-Pita JR, Martin GD, Hoath SD, et al. A simple large-scale droplet generator for studies of inkjet printing. *Rev Sci Instrum.* 2008;79(7).
19. Derby B. Inkjet printing ceramics: From drops to solid. *J Eur Ceram Soc.* 2011;31(14):2543-2550.
20. Derby B. Inkjet Printing of Functional and Structural Materials: Fluid Property Requirements, Feature Stability, and Resolution. *Annu Rev Mater Res.* 2010;40(1):395-414.
21. Matsumoto Y, Kobayashi N and Kawamura H. KYOCERA Corp, 2017. Liquid discharge head and recording device. U.S. Patent Application 15/128,263.
22. Brook C, Ristea A, Walsh M, et al. Xaar Technology Ltd, 2017. Droplet deposition apparatus and method for manufacturing the same. U.S. Patent 9,566,786
23. Mueller J, Courty D, Spielhofer M, et al. Mechanical Properties of Interfaces in Inkjet 3D Printed Single- and Multi-Material Parts. *3D Print Addit Manuf.* 2017;4(4):193-199.
24. Gordon R. Trends in Commercial 3D Printing and Additive Manufacturing. *3D Print Addit Manuf.* 2015;2(2):89-90.
25. Mashaan NS, Ali AH, Karim MR, et al. A Review on Using Crumb Rubber in Reinforcement of Asphalt Pavement. *Sci World J.* 2014;2014(i):1-21.
26. Cetin A. Effects of Crumb Rubber Size and Concentration on Performance of Porous Asphalt Mixtures. *Int J Polym Sci.* 2013;2013:1-10.
27. Stringer J, Derby B. Formation and stability of lines produced by inkjet printing. *Langmuir.* 2010;26(12):10365-10372.